Inorg. Chem. **2004**, *43*, 8355–8360

Coordinated Hydrazone Ligands as Nucleophiles: Reactions of $Fe(papy)_2$

Aaron Wood, Wasim Aris, and David J. R. Brook*

Department of Chemistry and Biochemistry, University of Detroit Mercy, P.O. Box 19900, Detroit, Michigan 48219

Received June 4, 2004

The diamagnetic iron(II) complexes of the hydrazone ligand pyridinecarboxaldehyde-2′-pyridylhydrazone (papyH) have been characterized by NMR, IR, UV–vis, and electrochemistry. The dication $Fe(papyH)_2^{2+}$ undergoes reversible one-electron oxidation at 0.66 V vs internal ferrocene and shows a strong metal–ligand charge-transfer band in the visible region at 524 nm. Deprotonation with NaOH gives diamagnetic, neutral $Fe(papy)_2$ with an oxidation potential of –0.25 V vs internal ferrocene and a charge-transfer band at 603 nm. $Fe(papy)_2$ reacts with active alkylating agents to give dialkyl complexes $Fe(papyR)_2^{2+}$ with spectroscopic properties similar to those of $Fe(papyH)_2^{2+}$. Monitoring the alkylation by UV–vis reveals the intermediacy of a monoalkylated species.

Introduction

Terpyridine (terpy) ligands have become a staple of transition metal coordination chemistry, providing metal complexes with important magnetic, redox, photophysical, and photochemical properties.[1,2] Ligands based on terpyridine have also played an important role in the design of self-assembling systems, in particular in the formation of squares, grids, and other metal-linked geometric structures.[3] The hydrazone ligand 2-pyridinecarboxaldehyde-2′-pyridylhydrazone (papyH) also offers a terpyridine-like coordination environment, but upon coordination to metals the amine (NH) proton of the hydrazone becomes significantly more acidic and can be quantitatively removed with aqueous base.[4−8] The resulting anionic ligand remains coordinated to the metal, but the atoms (C and N) bearing the formal negative charge are not coordinated and are potential nucleophiles.[9] Recent results have demonstrated that suitably substituted hydrazones are capable of coordinating metals to give multimetallic square grid complexes[10−12] and the photophysical and chemical properties of these complexes can be modulated by controlling the degree of protonation of the ligands. To understand these complex systems, a more detailed investigation of the metal−hydrazone system is required. Furthermore, nucleophilic reactions of the coordinated hydrazone ligands in such systems may be an important route to the further assembly of nanoscale molecular clusters. To our knowledge, the only study of the nucleophilic chemistry of coordinated hydrazones involved the paramagnetic nickel complex $Ni(papy)_2$.[9] Its alkylation products were characterized through elemental analysis and infrared spectroscopy. Iron complexes of papyH are diamagnetic and thus easily studied by NMR, providing further information as to the chemical structure of the products of these reactions. In addition, iron complexes of ligands such as terpy frequently have interesting photophysical and magnetic properties;[13−20] an investigation into the reactivity of the iron−papyH complexes should provide

* Author to whom correspondence should be addressed. E-mail: brookd@udmercy.edu.

(1) Sauvage, J.-P.; Collin, J.-P.; Chanbron, J.-C.; Guillerez, S.; Coudret, C. *Chem. Rev.* **1994**, *94*, 993−1019.
(2) Balzani, V.; Juris, A.; Venturi, M.; Campagna, S.; Serroni, S. *Chem. Rev.* **1996**, *96*, 759−833.
(3) Lehn, J. M. *Supramolecular Chemistry*; VCH: Weinheim, Germany, 1995.
(4) Geldard, J. F.; Lions, F. *Inorg. Chem.* **1963**, *2*, 270.
(5) Taya, T.; Sakamoto, T.; Doi, K.; Otomo, M. *Bull. Chem. Soc. Jpn.* **1993**, *66*, 3652−3661.
(6) Green, R. W.; Goodwin, W. G. *Aust. J. Chem.* **1968**, *21*, 1165.
(7) Green, R. W.; Hallman, P. S.; Lions, F. *Inorg. Chem.* **1964**, *3*, 376.
(8) Chiswell, B.; Lions, F.; Geldard, J. F.; Phillip, A. T. *Inorg. Chem.* **1964**, *3*, 1272.
(9) Black, D. S.; Srivastava, R. C. *Aust. J. Chem.* **1971**, *24*, 287−293.
(10) Uppadine, L. H.; Gisselbrecht, J. P.; Lehn, J. M. *Chem. Commun.* **2004**, 718−719.
(11) Uppadine, L. H.; Lehn, J. M. *Angew. Chem., Int. Ed.* **2004**, *43*, 240−243.
(12) Ruben, M.; Lehn, J. M.; Vaughan, G. *Chem. Commun.* **2003**, 1338−1339.
(13) Kimura, M.; Horai, T.; Muto, T.; Hanabusa, K.; Shirai, H. *Chem. Lett.* **1999**, 1129.
(14) Wilson, L. J.; Georges, D.; Hoselton, M. A. *Inorg. Chem.* **1975**, *14*, 2968.
(15) Ayers, T.; Scott, S.; Goins, J.; Caylor, N.; Hathcock, D.; Slattery, S. J.; Jameson, D. L. *Inorg. Chim. Acta* **2000**, *307*, 7−12.
(16) Priimov, G. U.; Moore, P.; Maritim, P. K.; Butalanyi, P. K.; Alcock, N. W. *J. Chem. Soc., Dalton Trans.* **2000**, 445−449.

10.1021/ic0492688 CCC: $27.50
Published on Web 11/12/2004

some insight into their use in constructing larger supramolecular or self-assembling systems.

Experimental Section

General. The ligand papyH was synthesized from the respective aldehyde and hydrazine as reported by Bell and Rose[21] and was recrystallized from ethanol. NMR spectra were recorded on a JEOL Eclipse 300+ 300 MHz Fourier transform spectrometer. Chloroform-*d* was stored over anhydrous potassium carbonate. Infrared spectra were recorded on a Perkin-Elmer Spectrum 2000 FTIR spectrometer. Spectra were measured either by diffuse reflectance on a sample dispersed in a KBr powder or by transmittance of a thin film of sample on a NaCl plate. Electrospray mass spectra were recorded with an Agilent 1100 series ion trap mass spectrometer equipped with an electrospray ion source. UV−vis spectra were recorded with an Ocean Optics PC2000 diode array spectrophotometer using a combination tungsten filament/deuterium lamp light source. Electrochemistry was performed with a Gamry PCI4 potentiostat, platinum disk working electrode, platinum wire counter electrode, and Ag/Ag^+ reference electrode. Tetrabutylammonium perchlorate was used as supporting electrolyte, and ferrocene was used as an internal standard. Acetonitrile for electrochemical experiments was distilled from calcium hydride.

Fe(papy)$_2$. A solution of ferrous ammonium sulfate hexahydrate (392 mg, 1 mmol) in 2 mL of water was added to a hot solution of papyH (398 mg, 2 mmol) in 20 mL of ethanol. A dark red color was immediately observed in solution, and upon cooling a red crystalline precipitate formed. Filtration gave crude $[Fe(papyH)_2]^{2+}SO_4^{2-}$, 483 mg, as a dark red crystalline solid contaminated with ammonium sulfate and Fe(III) compounds. Next, 450 mg of this solid was dissolved in hot water (40 mL)/methanol (20 mL), and 10 mL of 1 N aqueous NaOH was added. A dark brown-green precipitate formed immediately. After the solution was cooled, the product was removed by filtration. The crude product showed significant paramagnetic broadening of the ^{1}H NMR signal. Two recrystallizations from ethanol/water gave black-green needles, 166 mg, with ^{1}H NMR ($CDCl_3$) δ 6.13 (2H, t, $J = 6.3$), 6.51 (2H, t, $J = 6.3$), 6.74 (2H, d, $J = 8.25$), 7.04 (4H, m), 7.17 (4H, m), 7.44 (2H, d, $J = 5.5$), 9.08 (2H, s); ^{13}C NMR ($CDCl_3$) δ 109.2, 114.2, 117.6, 120.1, 133.0, 134.9, 136.5, 148.7, 151.6, 162.9, 170.9; ESMS $m/z = 451$ (100, Fe(papyH)(papy)$^+$); IR (NaCl plate) 3057, 1592, 1555, 1537, 1487, 1469, 1449, 1408, 1358, 1303, 1291, 1258, 1149, 1124, 1094, 1012, 760, 741, 702 cm^{-1}; UV−vis (MeCN) 603 (5900), 485 (17 400), 395 (39 000), 335 (sh, 16 000).

[Fe(papyH)$_2$](BF$_4$)$_2$. Fe(papy)$_2$ (22 mg) was dissolved in 1 mL of acetonitrile, and 48% aqueous HBF_4 was added dropwise until the solution turned from green-brown to red (ca. 1 drop). Evaporation of the solution gave the tetrafluoroborate salt as a red solid with ^{1}H NMR (CD_3CN) δ 9.43 (s, 2H), 7.81 (2H, d, $J = 7.7$), 7.74 (2H, t, $J = 9.2$), 7.68 (2H, t, $J = 5.5$), 7.583 (2H, t, $J = 8.5$), 7.49 (2H, d, $J = 5.2$), 7.07 (2H, t, $J = 5.5$), 7.00 (2H, d, $J = 8.5$), 6.74 (2H, t, $J = 7.0$); ^{13}C NMR (CD_3CN) δ 159.3, 157.7, 152.8, 149.5, 145.7, 140.5, 138.5, 126.0, 125.0, 119.9, 107.5; ESMS $m/z = 451$ (100, Fe(papyH)(papy)$^+$), 226 (11, Fe(papyH)$_2^{2+}$); IR (NaCl plate) 3293, 1620, 1603, 1581, 1547, 1461, 1149, 1065, 766 cm^{-1}; UV−vis (MeCN) 522 (7450), 463 (4800), 330 (45 000). Anal. Calcd for $C_{22}H_{18}B_2F_8FeN_8 \cdot 3H_2O$: C, 38.86; H, 3.83; N, 16.48. Found: C, 38.93; H, 3.55; N, 16.02.

[Fe(papy−CH$_3$)$_2$]I$_2$. Fe(papy)$_2$ (22 mg) was dissolved in 1 mL of CH_3I, and after being stirred for 30 min the solution was allowed to stand for 24 h. Filtration gave 24 mg (67%) of Fe(papy−CH_3)$_2$I$_2$ as a red precipitate with ^{1}H NMR (D_2O) δ 4.37 (6H, s), 6.74 (2H, t, $J = 7.4$), 7.05 (2H, t, $J = 6.3$), 7.11 (2H, d, $J = 8.2$), 7.54 (2H, d, $J = 5.2$), 7.7 (6H, m), 7.85 (2H, $J = 7.5$), 9.48 (2H, s); ^{13}C NMR (DMSO-d_6) 159.6, 157.9, 153.2, 151.0, 143.8, 141.3, 139.1, 126.7, 125.5, 120.7, 108.5, 35.8; IR (NaCl plate) 1599, 1567, 1530, 1491, 1458, 1434, 1315, 1236, 1204, 1147, 1101, 1019, 989, 760 cm^{-1}; ESMS $m/z = 240$ (100, Fe(papy−CH_3)$_2^{2+}$); UV−vis (water) 524 nm (6900), 466 nm (4100), 390 (sh, 15 600). Anal. Calcd for $C_{24}H_{24}FeI_2N_8 \cdot 2H_2O$: C, 37.41; H, 3.64; N, 14.55. Found: C, 37.00; H, 3.55; N, 14.04.

[Fe(papy−CH$_2$CH=CH$_2$)$_2$]Br$_2$. Fe(papy)$_2$ (150 mg) was dissolved in 2 mL of dichloromethane, and a large excess (2 mL) of allyl bromide was added. The resulting solution was allowed to stand at room temperature for 24 h, during which time red needles precipitated. Filtration gave 149 mg of crude Fe(allylpapy)$_2$Br$_2$, which was further purified by recrystallization from acetonitrile. ^{1}H NMR (D_2O) δ 9.51 (s, 2H), 7.84 (d, 2H, $J = 8$), 7.74 (t, 2H, $J = 7.68$), 7.68 (t, 2H, $J = 8.8$), 7.63 (d, 2H, $J = 5.2$), 7.56 (d, 2H, $J = 5.2$), 7.14 (d, 2H, $J = 8.5$), 7.08 (t, 2H, $J = 6$), 6.82 (t, 2H, $J = 6.5$), 6.354 (m, 2H), 5.74 (d, 2H, $J = 17.5$), 5.69 (d, 2H, $J = 10.7$), 5.54 (d, 4H, $J = 3.8$); ^{13}C NMR (D_2O) δ 49.89, 108.21, 120.39, 120.43, 125.37, 126.09, 128.41, 138.40, 140.89, 143.01, 149.96, 152.19, 157.45, 159.07; IR (NaCl plate) 1600, 1569, 1533, 1484, 1446, 1327, 1185, 1162, 1148, 1108, 832, 767 cm^{-1}; ESMS $m/z = 491$ (100, Fe(papy)(papy−C_3H_5)$^+$), 266 (58, Fe(papy−C_3H_5)$_2^{2+}$), 245.5 (20, Fe(papy)(papy−C_3H_5)$^{2+}$); collision-induced fragmentation of the ion at $m/z = 491$ resulted in further loss of allyl radical to give $m/z = 450$. Similarly, fragmentation of the $m/z = 266$ ion resulted in a fragment at 245.5 corresponding to loss of allyl radical.

[Fe(papy−CH$_2$−*p*-C$_6$H$_4$Br)$_2$](PF$_6$)$_2$. To 20 mg of Fe(papy)$_2$ dissolved in 2 mL of CH_2Cl_2 was added 2 mol equiv of 4-bromobenzyl bromide. The solution was allowed to stand at room temperature for 2 days, and the resulting red-brown solution was layered with heptane. This precipated 40 mg of the crude benzylated complex. Further purification was achieved by dissolution in methanol and precipitation with ammonium hexafluorophosphate, followed by recrystallization by vapor diffusion of ether into an acetonitrile solution. The resulting red solid had a ^{1}H NMR spectrum severely broadened by paramagnetic impurities; however, other spectral data (described below) were consistent with the proposed structure. ^{13}C NMR (methanol-d_4) 159.2, 158.3, 152.5, 150.4, 144.4, 141.6, 138.8, 133.1, 132.8, 129.9, 126.7, 126.2, 122.6, 121.1, 108.7, 50.8; ESMS $m/z = 395$ (100, [Fe(papy−CH_2−*p*-$C_6H_4Br)_2$]$^{2+}$); IR (NaCl plate) 3098, 1605, 1574, 1535, 1486, 1466, 1450, 1411, 1326, 1250, 1176, 1106, 1072, 1011, 842, 766.

[Fe(papy−CH$_2$−*p*-C$_6$H$_4$−CH$_2$Br)$_2$](PF$_6$)$_2$. To 20 mg of Fe(papy)$_2$ dissolved in 2 mL of CH_2Cl_2 was added 4 mol equiv of *p*-xylylene dibromide. The solution was allowed to stand at room temperature for 2 days, and the resulting red-brown solution was layered with heptane. This precipated 72 mg of the crude alkylated complex. Further purification was achieved by dissolution in methanol and precipitation with ammonium hexafluorophosphate, followed by recrystallization by vapor diffusion of ether into an acetonitrile solution. The resulting red solid had a ^{1}H NMR spectrum severely broadened by paramagnetic impurities; however,

(17) McCusker, J. K.; Walda, K. N.; Dunn, R. C.; Simon, J. D.; Magde, D.; Hendrickson, D. N. *J. Am. Chem. Soc.* **1993**, *115*, 298−307.
(18) Renz, F.; Oshio, H.; Ksenofontov, V.; Waldeck, M.; Spiering, H.; Gutlich, P. *Angew. Chem., Int. Ed.* **2000**, *39*, 3699−3700.
(19) Ruben, M.; Breuning, E.; Lehn, J. M.; Ksenofontov, V.; Renz, F.; Gutlich, P.; Vaughan, G. B. M. *Chem.-Eur. J.* **2003**, *9*, 4422−4429.
(20) Breuning, E.; Ruben, M.; Lehn, J. M.; Renz, F.; Garcia, Y.; Ksenofontov, V.; Gutlich, P.; Wegelius, E.; Rissanen, K. *Angew. Chem., Int. Ed.* **2000**, *39*, 2504.
(21) Bell, C. F.; Rose, D. R. *J. Chem. Soc. A* **1969**, 988.

other spectral data (described below) were consistent with the proposed structure. ^{13}C NMR (methanol-d_4) 159.2, 158.3, 152.4, 150.3, 144.2, 141.5, 139.6, 138.8, 133.7, 130.5, 128.6, 126.7, 126.1, 121.0, 108.9, 50.7, 32.9; ESMS m/z = 409 ([Fe(papy−CH_2−p-C_6H_4−$CH_2Br)_2$]$^{2+}$), 963 ([Fe(papy−CH_2−p-C_6H_4−$CH_2Br)_2$]-(PF_6)$^+$) (relative intensities not reported because peaks were observed over different scan ranges); IR (NaCl plate) 1604, 1574, 1534, 1485, 1466, 1449, 1422, 1400, 1324, 1250, 1160, 1105, 1054, 1028, 1010, 842, 767.

[Fe(papy−CH_2COOEt)$_2$]Br$_2$. To 150 mg of Fe(papy)$_2$ dissolved in 10 mL of CH_2Cl_2 was added an excess (1 mL) of ethyl bromoacetate. The solution was allowed to stand at room temperature, during which the solution turned from green-brown to red. After the solution was left standing for 2 days, dark red crystals precipitated. These were removed by filtration to give 238 mg of Fe(papy−CH_2COOEt)$_2$Br$_2$ with ^{1}H NMR (D_2O) δ 9.54 (s, 2H), 7.8 (complex multiplet, 10H), 7.11 (m, 4H), 6.86 (t, 2H), 5.87 (s, 4H), 4.47 (q, 4H, J = 7), 1.39 (t, 6H, J = 7); ^{13}C NMR 168.4, 158.7, 157.1, 152.6, 150.5, 143.3, 141.1, 138.5, 126.4, 125.8, 120.8, 107.7, 64.1, 47.9, 13.6; ESMS m/z = 312 (100, Fe(papy−CH_2COOEt)$_2^{2+}$), 703 (50, Fe(papy−CH_2COOEt)$_2$Br$^+$); IR (NaCl plate) 2992, 1737, 1603, 1574, 1537, 1488, 1466, 1449, 1327, 1228, 1116, 1019, 765.

Kinetics. Kinetic measurements were performed on acetonitrile solutions of Fe(papy)$_2$ containing a large excess of methyl iodide to give pseudo-first-order kinetics. The sample temperature was maintained at 25 °C with a recirculating temperature controlled bath, and the UV−vis spectrum was measured at regular time intervals with the Ocean Optics spectrophotometer described above. Data were analyzed with MATLAB using an algorithm similar to that described by Atkins et al. for analysis of equilibria.[22] An initial guess of the rate constants gives a concentration profile that can be used to extract, through linear least squares, approximate component spectra. Adjusting the rate constants to minimize the difference between the least squares solution and actual spectra gives optimized rate constants along with spectra of intermediate species.

Computational Studies. Ab initio molecular orbital calculations were performed using the GAMESS[23] software package running under Macintosh OSX. Structures of papyH and papy$^-$ were optimized with the 3-21G basis set, and subsequently molecular orbitals were calculated with the 6-31G** basis set. Orbitals were visualized with MacMolPlt.[24]

Results

Our synthesis of the iron complexes of papy followed literature procedures. The combination of the ligand and ammonium iron(II) sulfate in ethanol/water gives an initial papyH salt that can be subsequently deprotonated with bases to give the neutral, organic soluble, papy complex (Scheme 1).

Following this route, we found that initial samples of Fe(papyH)$_2^{2+}$ salts and samples of Fe(papy)$_2$ were contaminated with paramagnetic (probably iron(III)) impurities. Fortunately, we found that these can be removed from

Scheme 1

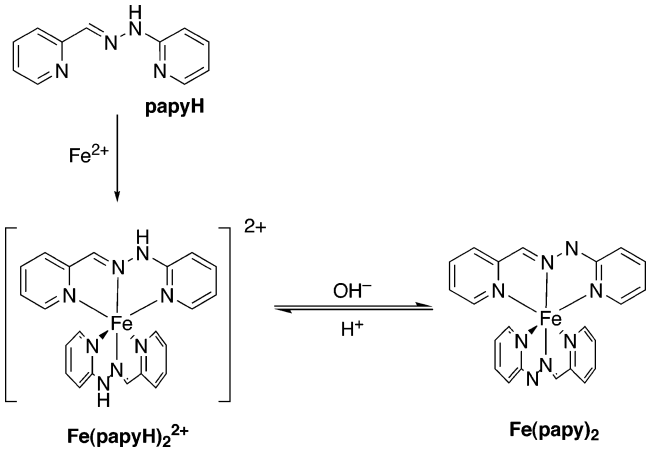

Fe(papy)$_2$ by repeated hot filtration/recrystallization from ethanol/water. Fe(papyH)$_2^{2+}$ and other species were then synthesized from the purified neutral compound.

Fe(papy)$_2$ has been described several times previously in the literature, although these characterizations were based on UV−vis spectra and elemental analysis.[4,25] In particular, previous studies report Fe(papy)$_2$ as a paramagnetic substance (vide supra). We find that solutions of sufficiently purified samples are diamagnetic, and both Fe(papy)$_2$ and Fe(papyH)$_2^{2+}$(BF_4^-)$_2$ give well-resolved ^{1}H and ^{13}C NMR spectra. Assignment of resonances via two-dimensional pulse sequences reveals some notable differences between these and the free ligand. In particular, upon coordination, the imine CH proton moves downfield from 7.95 to 9.7 ppm while the protons in the 6 and 6′ positions move upfield; subsequent deprotonation moves all resonances upfield by ∼0.7 ppm. NMR spectra of the three species papyH, Fe(papyH)$_2^{2+}$, and Fe(papy)$_2$ in acetonitrile are shown in Figure 1.

Previous studies reported the UV−vis spectra of Fe(papyH)$_2^{2+}$ and Fe(papy)$_2$. Our studies are consistent with these reports but provide additional details. Fe(papyH)$_2^{2+}$ is deep red and shows a long wavelength absorption at 524 nm (ϵ = 6900), while solutions of Fe(papy)$_2$ are green-brown and show a long wavelength absorption maximum at 603 nm (ϵ = 4050). Further inspection also reveals a low intensity absorption tail that extends out to 850 nm. N-Alkylated derivatives of Fe(papy)$_2$ (vide infra) show UV−vis spectra similar to that of Fe(papyH)$_2^{2+}$. Unlike other reported papy complexes,[25] we see no evidence of dichroism for the compounds reported here.

Although one paper describes the electrochemical synthesis of Fe(papy)$_2$,[25] the electrochemistry of these complexes themselves has not been previously reported. In acetonitrile, both Fe(papy)$_2$ and Fe(papyH)$_2$ are oxidized by one electron in quasi-reversible processes: the oxidation of Fe(papyH)$_2$ occurs at 0.66 V vs ferrocene/ferricinium (Fc/Fc$^+$), while Fe(papy)$_2$ is oxidized at the considerably lower potential of −0.25 V vs Fc/Fc$^+$. No evidence was found for the reversible reduction of either complex.

(22) Atkins, C. E.; Park, S. E.; Blaszak, J. A.; McMillin, D. R. *Inorg. Chem.* **1984**, *23*, 569−572.
(23) Schmidt, M. W.; Baldridge, K. K.; Boatz, J. A.; Elbert, S. T.; Gordon, M. S.; Jensen, J. H.; Koseki, S.; Matsunaga, N.; Nguyen, K. A.; Su, S. J.; Windus, T. L.; Dupuis, M.; Montgomery, J. A. *J. Comput. Chem.* **1993**, *14*, 1347−1363.
(24) Bode, B. M.; Gordon, M. S. *J. Mol. Graphics Modell.* **1998**, *16*, 133−138.
(25) Vecchio-Sadus, A. M. *Transition Met. Chem.* **1995**, *20*, 256−261.

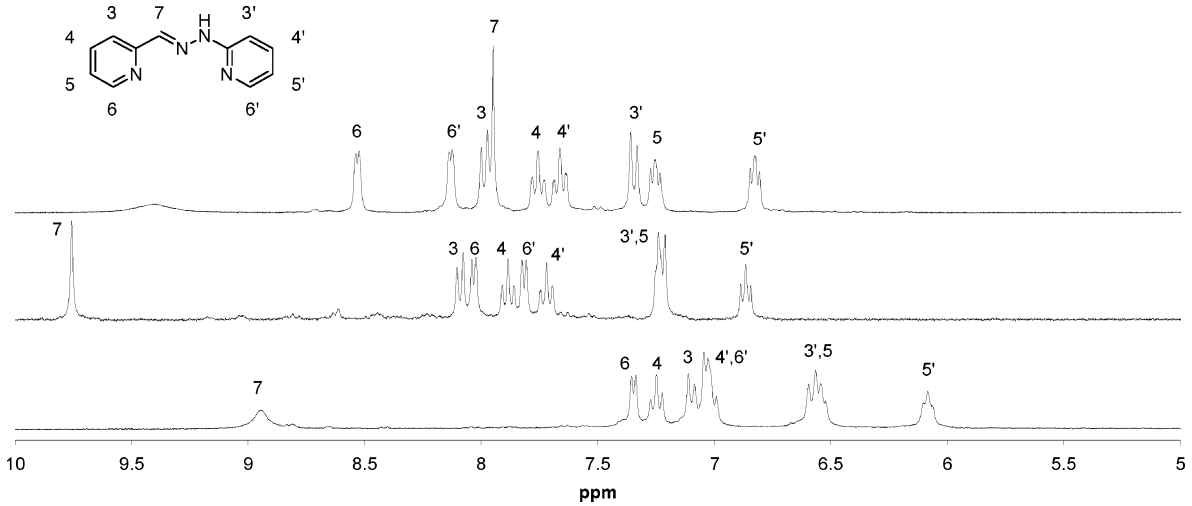

Figure 1. ^{1}H NMR spectra of papyH (top), $[Fe(papyH)_2]^{2+}(BF_4^-)_2$ (middle), and $Fe(papy)_2$ (bottom) in acetonitrile-d_3. The structure indicates the numbering used for peak assignments.

Scheme 2

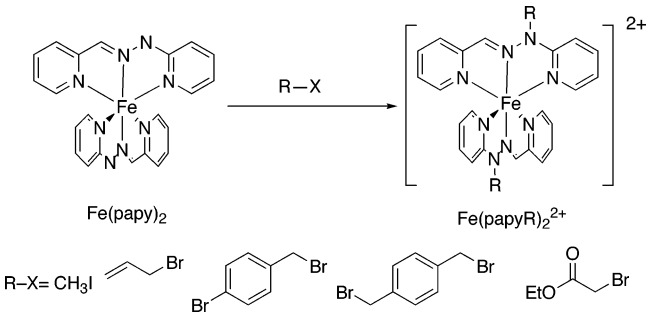

The combination of $Fe(papy)_2$ with reactive alkyl halides (methyl iodide, allyl bromide, ethyl bromoacetate, benzylic bromides) in acetonitrile or dichloromethane results in the formation of the corresponding red, alkylated complexes (Scheme 2). Spectroscopic properties of these species are similar to those of $Fe(papyH)_2^{2+}$. Reaction with alkyl halides capable of elimination, acyl halides, and acid anhydrides, however, gave complex mixtures of products whose composition was not determined. Comparable reactions with $Ni(papy)_2$ gave compounds identified as mixed ligand complexes.[9] The requirement for simple, reactive halides is understandable based on the fact that $Fe(papy)_2$ is a rather hindered, weakly basic (pK_a ($Fe(papyH)_2^{2+}$) = 5.68, 6.57)[7] nucleophile.

Monitoring the methylation of $Fe(papy)_2$ under pseudo-first-order conditions (excess methyl iodide) in acetonitrile by UV−vis showed initial formation of an intermediate species (presumably the monoalkyl product) followed by a slower second alkylation forming the dialkyl species (Figure 2).

Fitting of the spectral region between 425 and 850 nm to a consecutive pseudo-first-order model gave rate constants of $2.7(1) \times 10^{-3}$ and $0.19(1) \times 10^{-3}$ L mol^{-1} s^{-1} (corrected for CH_3I concentration) for the first and second alkylations, respectively. The regression procedure also gave the spectrum for the intermediate monoalkylated species (Figure 3).

The monomethyl complex shows a maximum at 580 nm, partway between $Fe(papy)_2$ and $Fe(papy\text{-}CH_3)_2^{2+}$, and a truncated long wavelength absorption tail that ends at 750 nm but is somewhat more intense than that for $Fe(papy)_2$.

Discussion

The oxidation potential for $Fe(papyH)_2^{2+}$ (0.66 V vs Fc/Fc^+) is somewhat less than that for $Fe(terpy)_2^{2+}$ (0.895 V vs Fc/Fc^+ in DMF[26]) but is comparable to Fe^{2+} complexes of other imine ligands such as phen (0.75 V vs Fc/Fc^+) and bipy (0.59 V vs Fc/Fc^+).[27] The UV spectrum shows an MLCT transition similar to $Fe(terpy)_2^{2+}$ (λ_{max} = 560 nm[26]) but blue shifted by 40 nm. There is also an additional maximum at lower wavelength, similar to those observed by Krumholz in the iron complexes of other tridentate imine ligands.[28] These bands have been assigned to metal−ligand charge-transfer (MLCT) transitions.

Deprotonation gives the neutral, diamagnetic complex $Fe(papy)_2$. This complex was previously described as paramagnetic,[4,25] possibly as a result of impurities resulting from the facile one-electron oxidation (vide infra). The problem of impurities giving spurious magnetic data for iron(II) imine complexes has been previously noted.[29] In fact, measurements on some of our crude samples have given large paramagnetic susceptibilities and room-temperature ESR signals. Nevertheless, the variable susceptibility of solid samples observed by ourselves and others suggests that impurities are to blame.

The large reduction in oxidation potential (−0.91 V) upon deprotonation is noteworthy because similar changes in oxidation potential were recently utilized in constructing a mixed-valence molecular square based on cobalt and hydrazone ligands.[11] Deprotonation also results in a significant red shift of the UV−vis spectrum and an upfield shift of the ligand ^{1}H NMR resonances. These changes are best understood by examining the orbital structure of the ligand and

(26) Braterman, P. S.; Song, J. I.; Peacock, R. D. *Inorg. Chem.* **1992**, *31*, 555−559.
(27) *Encyclopedia of Electrochemistry of the Elements*; Marcel Dekker: New York, Basel, 1982; Vol. IX, part A.
(28) Krumholz, P. *Inorg. Chem.* **1965**, *4*, 612−616.
(29) Sinn, E. *Inorg. Chim. Acta* **1969**, *3*, 11−16.

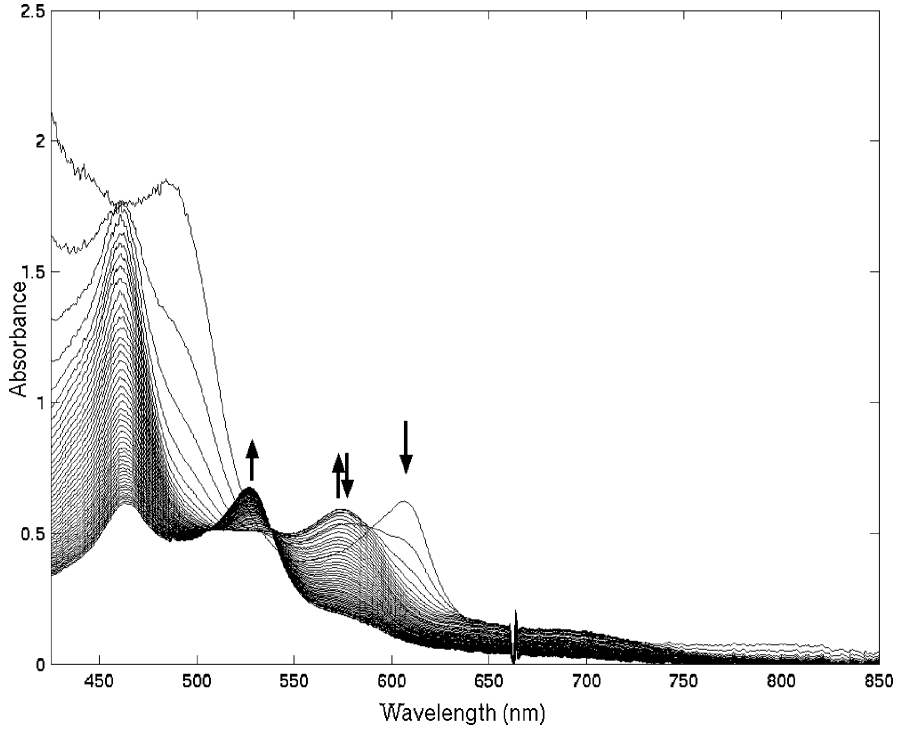

Figure 2. UV spectra recorded at 5 min intervals during the alkylation of $Fe(papy)_2$ with excess CH_3I.

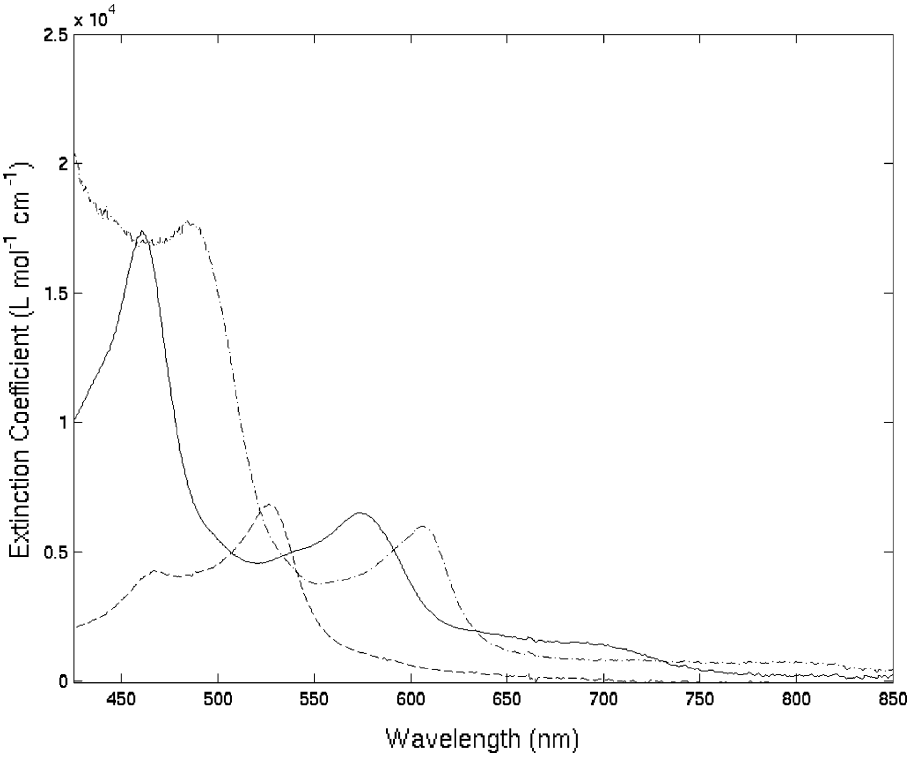

Figure 3. UV spectra of $Fe(papy)_2$ (— · —), $[Fe(papy\text{-}CH_3)(papy)]^+$ (—), and $[Fe(papy\text{-}CH_3)_2]^{2+}$ (- - -) from deconvolution of kinetic data.

its anion. Molecular orbital calculations show that both ligands are planar with the hydrazone N−H lying in the plane of the molecule to give a fully conjugated system. In the neutral ligand, the coordinating lone pair of the hydrazone unit corresponds to a σ orbital that has significant magnitude on the noncoordinating face of the ligand around the hydrazone C−H and N−H bonds. Coordinating the nitrogen to a metal center reduces the electron density in these bonds, resulting in the large downfield shift in the NMR of the CH and the increased acidity of the NH bond. Similar, but less pronounced, ^{1}H NMR shifts were observed in the corresponding zinc complexes.[30] Deprotonation of the N−H results in the formation of a high-energy σ orbital (HOMO−2 calculated using the 6-31G* basis set) that also extends across

(30) Bell, C. F.; Mortimore, G. R.; Reed, G. L. *Org. Magn. Reson.* **1976**, *8*, 45−48.

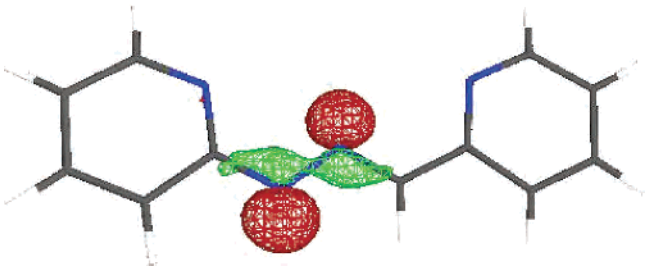

Figure 4. Highest occupied σ orbital of the papy$^-$ anion, calculated at the 6-31G* level.

the molecule with significant magnitude on the coordinating imine nitrogen (Figure 4).

This results in an increase in the σ donor strength of the ligand, increasing the electron density on the metal, and reducing the energy of the observed metal ligand charge-transfer band. The lower oxidation potential of the neutral complex, while consistent with the reduction in charge, may also be explained in part by the increase in electron density on the metal center. This model also accounts for the spectrum of the monoalkylated intermediate; with one anionic ligand, the metal donor orbitals are midway between the corresponding orbitals on the neutral and dicationic species, hence the MLCT transition is also midway between those of the neutral and dicationic species.

Alkylation of the $Fe(papy)_2$ complex can be achieved with a variety of active electrophiles; we have chosen a series that bear additional functionality, suggesting the possibility of further structural elaboration. With the methylation reaction, rate constants for the first and second alkylation only differ by a factor of 10. While this is enough to allow for an effective synthesis of monoalkylated product, the difference suggests that the reactivity of the nucleophilic site is not greatly affected by the other ligand. A similar effect was observed in the two pK_a values for this complex.[7] Also of note is the reaction with the two benzyl bromides. While the products of other alkylation reactions were clearly diamagnetic, the benzylated derivatives showed strongly broadened ^{1}H NMR data even when reactions were performed under nitrogen. While these molecules may be inherently paramagnetic, we feel this is unlikely considering the other alkylated products. The remaining spectra were entirely consistent with the proposed structures, so we believe a more likely explanation for this paramagnetic broadening is the introduction of small amounts of high-spin impurities, possibly through ligand exchange reactions. Analogous reactions with benzyl chloride and $Ni(papy)_2$ apparently resulted in the disruption of the metal complex and coordination of chloride to the metal center.[9]

Conclusion

$Fe(papy)_2$ and $Fe(papyH_2)^{2+}$ have been known for over 40 years; nevertheless, their characterization and chemistry has only barely been investigated. We have found that the $Fe(papyH)_2^{2+}$ cation is quite similar to $Fe(terpy)_2^{2+}$ in several respects and that the changes in chemistry occurring upon deprotonation can be understood in terms of the change in ligand electronic structure. This understanding will undoubtedly be important in describing the spectroscopic behavior of the recently reported hydrazone ligand-based molecular squares. In addition, $Fe(papy)_2$ acts as a bis-nucleophile, allowing the introduction of a variety of reactive organic functional groups without disrupting the central metal complex. This suggests the possibility of building a variety of more elaborate complexes based on the $Fe(papy)_2$ unit.

Acknowledgment. This work was funded in part by the Petroleum Research Fund, Grant 39923-B1, to D.J.R.B. and the National Science Foundation Grants DUE-ILI-9851311 and MRI-0116181 for the purchase of NMR and LC-MS instruments. We also thank Dr. Gordon Yee for magnetic susceptibility measurements.

Supporting Information Available: Detailed description of the algorithm used to fit the kinetic data, ^{1}H and ^{13}C NMR spectra for $Fe(papy)_2$, $Fe(papyH)_2(BF_4)_2$, $Fe(papy-CH_3)_2I_2$, $Fe(papy-C_3H_5)_2Br_2$, $Fe(papy-CH_2CO_2Et)_2Br_2$, and ^{13}C NMR spectra for $Fe(papy-CH_2C_6H_4Br)_2(PF_6)_2$ and $Fe(papy-CH_2-C_6H_4CH_2Br)_2(PF_6)_2$. This material is available free of charge via the Internet at http://pubs.acs.org.

IC0492688